Published in "Journal of the Physical Society of Japan 79: 104705 , 2010"
which should be cited to refer to this work.

Phase Transition in the 3-Kelvin Phase of Eutectic Sr_2RuO_4–Ru

Hirono KANEYASU[1,3*], Nobuhiko HAYASHI[2,3], Bruno GUT[4],
Kenji MAKOSHI[1,3], and Manfred SIGRIST[5]

[1]*Department of Material Science, University of Hyogo, Kamigori, Hyogo 678-1297, Japan*
[2]*Nanoscience and Nanotechnology Research Center (N2RC), Osaka Prefecture University, Sakai 599-8570, Japan*
[3]*CREST(JST), Kawaguchi, Saitama 332-0012, Japan*
[4]*Department of Physics, University of Fribourg, Chemin du Musée 3, 1700 Fribourg, Switzerland*
[5]*Theoretische Physik, ETH-Zürich, Zürich CH-8093, Switzerland*

The inhomogeneous 3-Kelvin (3K) phase of the eutectic Sr_2RuO_4 with Ru inclusions nucleates superconductivity at the interface between Ru and Sr_2RuO_4. The structure of the interface state and its physical properties are examined here. Two superconducting phases are identified between the transitions to the bulk phase at 1.5 K and to the 3K phase. The nucleation of the 3K phase results in a state conserving time reversal symmetry, which generates an intrinsically frustrated superconducting network in samples with many Ru inclusions. At a lower temperature (>1.5 K), a discontinuous (first order) transition to an interface state breaking time reversal symmetry is found leading to an unfrustrated network phase. It is shown that this phase transition located at a temperature between 1.5 and 3 K would yield the anomalous property showing that the critical current in such a network depends on the sign of the current, reproducing recent experimental observations.

KEYWORDS: unconventional superconductivity, chiral *p*-wave, Sr_2RuO_4, 3K phase

1. Introduction

Sr_2RuO_4 is a quasi-two-dimensional strongly correlated metal showing unconventional superconductivity with a bulk critical temperature $T_c^b = 1.5$ K.[1,2] There is strong evidence that the superconducting phase has a spin-triplet odd-parity character and breaks time reversal symmetry. The most likely order parameter has a chiral p-wave symmetry corresponding to a pairing state with the orbital structure $k_x \pm ik_y$ and the triplet spin configuration corresponding to $S_z = 0$. This state is usually represented by the vector gap function $\boldsymbol{d}(\boldsymbol{k}) = \hat{z}(k_x \pm ik_y)$ and is described as a two-component order parameter, for example as $\boldsymbol{d}(\boldsymbol{k}) = \eta_x \hat{z}k_x + \eta_y \hat{z}k_y$.

Some years ago, an intriguing feature of Sr_2RuO_4–Ru eutectic samples was discovered. Some of the Ru segregates into μm-sized inclusions embedded within the parent material Sr_2RuO_4. These samples show an onset to inhomogeneous superconductivity at approximately $T^* \approx 3$ K, which turns into the bulk superconducting phase at $T = T_c^b$.[3,4] This higher-temperature phase ($T_c^b < T < T^*$) has been called the "3-Kelvin" phase (3K phase). The early suggestion that the superconductivity in the 3K phase has filamentary nature, nucleating at the interface between Ru-inclusion and Sr_2RuO_4,[5] receives strong support on the basis of the behavior of the upper critical fields H_{c2}, which is enhanced and shows a characteristic sublinear dependence on $|T - T^*|$.[4,6] This theory is based on the assumption that, for some as-yet unknown reason, the pairing interaction is enhanced in Sr_2RuO_4 in the vicinity of the interface.[5] Interestingly, the effective symmetry lowering at the interface implies the nucleation of a superconducting state, which is different from that of the bulk state of Sr_2RuO_4 and does not violate time reversal symmetry. For the two-dimensional order parameter space of the p-wave state, i.e., $\boldsymbol{d}(\boldsymbol{k}) = \eta_x \hat{z}k_x + \eta_y \hat{z}k_y$, quite general arguments lead to the conclusion that the pairing state with the orbital symmetry $\boldsymbol{k} \cdot \boldsymbol{n} = 0$ (the p-wave lobe parallel to the interface) is realized at $T = T^*$ ($\boldsymbol{n}$ is the normal vector of the interface).[5] Consequently, the transition from the 3K phase to the bulk superconducting (chiral p-wave) phase is not merely a percolation transition as in the case of conventional inhomogeneous superconductors. At least, time reversal symmetry breaking (TRSB) has to occur on the way to the bulk phase.

In this study, we investigate the evolution of the 3K phase towards the bulk superconducting phase of Sr_2RuO_4 in the temperature range $T_c^b < T < T^*$. In this context, we will discuss three different phases for a closed interface of a Ru inclusion, which we call the A-, A′-, and B-phases. The A-phase appears at T^* and is time-reversal-conserving. At lower temperatures, a transition to a time-reversal-symmetry-violating phase named A′-phase (B-phase) occurs, which may have the same (different) topology as the A-phase. We will show that the A- and A′-phases introduce phase frustration, if we consider a network formed by the superconducting interfaces states of many Ru inclusions.[5] On the other hand, the topology of the B-phase yields a non-frustrated network. Our investigation shows that the additional transition is of first order from the A-phase to the B-phase; it breaks time reversal symmetry and simultaneously changes the topology of the states on an inclusion. The B-phase is then topologically identical to the bulk phase, which is eventually reached by percolation. The additional transition is accompanied by observable effects such as characteristic features of quasiparticle tunneling[7–10] and critical current.[11]

2. Model Formulation

To illustrate the most relevant features of the 3K phase, we first consider a single Ru inclusion modeled as a cylinder of radius R whose central axis lies along the z-axis of the tetragonal crystal lattice of Sr_2RuO_4. Here, we focus on the

*E-mail: hirono@sci.u-hyogo.ac.jp

superconductivity in the two-dimensional x–y plane and use the in-plane p-wave spin-triplet pairing as the dominant superconducting instability. Assuming for the bulk phase the chiral p-wave spin-triplet state, we represent the order parameter by the vector gap function as $\boldsymbol{d}(\boldsymbol{r},\boldsymbol{k}) = \eta_+(\boldsymbol{r})\hat{z}(k_x + \mathrm{i}k_y) + \eta_-(\boldsymbol{r})\hat{z}(k_x - \mathrm{i}k_y)$. With this order parameter, we now write a Ginzburg–Landau (GL) free energy for the region belonging to Sr_2RuO_4 around a single cylindrical Ru inclusion ($r > R$),

$$F = f_0 \int_{r>R} \mathrm{d}^3 r \Big[\tau(r)|\boldsymbol{\eta}|^2 + \frac{1}{6}\{|\boldsymbol{\eta}|^4 + 2|\eta_+|^2|\eta_-|^2\} + \{|\boldsymbol{D}\eta_+|^2 + |\boldsymbol{D}\eta_-|^2\} + 2\kappa^2(\nabla \times \boldsymbol{A})^2 + \frac{1}{2}\{(D_-\eta_+)^*(D_+\eta_-) + \text{c.c.}\}\Big]. \quad (1)$$

We use dimensionless units for our formulation, and the notation $\boldsymbol{\eta} = (\eta_+, \eta_-)$, $\tau(r) = T/T_c(r) - 1$. With the r-dependence of the critical temperature $T_c(r)$, we incorporate the local enhancement of the pairing interaction. We introduce the operators $\boldsymbol{D} = \nabla - i\boldsymbol{A}$ with $D_\pm = D_x \pm \mathrm{i}D_y$ and $\boldsymbol{A}$ as the dimensionless vector potential. The units are chosen so that the zero-temperature coherence length ξ_0 is the unit length, the order parameter reaches $|\eta_+|^2$ or $|\eta_-|^2 = -\tau$ in the uniform bulk state below T_c^b (2-fold degenerate state), and the vector potential is given in units of $\Phi_0/2\pi\xi_0$ ($\Phi_0 = hc/2e$ is the flux quantum). Moreover, κ is the usual GL parameter and f_0 is the free energy per unit volume. A straightforward variational calculation shows that the coordinate separation of the order parameter in eq. (1) is adequate here with N as the quantum number characterizing different topological sectors of the order parameter [see eq. (3)].

In order to model the narrow region of enhanced superconductivity at the interface, we introduce the spatially dependent $T_c(r)$ in the following form:

$$T_c(r) = T_c^b + \frac{T_0}{\cosh[(r-R)/d]} \quad \text{for } r \geq R. \quad (2)$$

Here, d is the width of the region close to the interface where T_c is locally enhanced with a maximum $T_c^b + T_0$ at the interface. At this moment, we ignore the magnetic field ($\boldsymbol{A} = 0$) and investigate first the nucleation of superconductivity.

With the given geometry and order parameter choice, it is advantageous to turn to cylindrical coordinates (r, θ, z). The GL equations allow to separate the dependences of the order parameters in radial and azimuthal coordinates into the form (assuming homogeneity along the z-axis),

$$\eta_\pm(\boldsymbol{r}) = \eta_\pm(r)\mathrm{e}^{\mathrm{i}(N\mp1)\theta}, \quad (3)$$

where N is an integer corresponding to the phase winding number of $\boldsymbol{d}(\boldsymbol{r},\boldsymbol{k})$ around the cylinder, since the order parameter is single-valued. This representation reflects the cylindrical symmetry of our model geometry and gives rise to the following symmetry properties. One finds $\boldsymbol{d} \to \boldsymbol{d}\exp(\mathrm{i}N\gamma)$ for a rotation of the system, $\theta \to \theta + \gamma$ and $\theta_k \to \theta_k + \gamma$, owing to the factor $k_x \pm \mathrm{i}k_y \equiv |\boldsymbol{k}|\exp(\pm\mathrm{i}\theta_k)$ and the phase factor of eq. (3). Here, we always keep the orientation of the $\boldsymbol{d}$ vector fixed parallel to the z-axis. The formulation of the boundary conditions is most conveniently performed with the radial and azimuthal components of the order parameter defined as

$$\eta_r(r,\theta) = \frac{1}{\sqrt{2}}[\eta_+(r) + \eta_-(r)]\mathrm{e}^{\mathrm{i}N\theta},$$
$$\eta_\theta(r,\theta) = \frac{\mathrm{i}}{\sqrt{2}}[\eta_+(r) - \eta_-(r)]\mathrm{e}^{\mathrm{i}N\theta}. \quad (4)$$

These two order parameters are differently affected by boundary effects due to their interference effects under surface scattering. These effects can be implemented by using the following standard boundary condition at the interface ($r = R$);

$$\left.\frac{\mathrm{d}\eta_\mu}{\mathrm{d}r}\right|_{r=R} = \frac{\eta_\mu(R)}{\ell_\mu}, \quad (5)$$

where μ stands for "r" or "θ". Here, ℓ_μ is the so-called extrapolation length characterizing the boundary effect for each component (for example, see, ref. 12). We assume $\ell_\theta \to \infty$, since the tangential component of a Cooper pair wave function at an interface is not affected by (specular) surface scatterings.[13] On the other hand, there is a suppression of the radial component (sign change order parameter under reflection at the interface) requiring a finite value of ℓ_r. In our model, we neglect the superconducting component induced in the Ru inclusion, assuming an interface of very low transmissivity, consistent with our assumption of the boundary condition. This model will now be used to derive a phase diagram of the 3K phase.

3. Phases and Phase Diagram

For given N and T, we can now determine the r dependence of the order parameter by varying the GL free energy including the boundary conditions. We find three states which are of interest for the discussion of the 3K phase, which we named the A-, A′-, and B-phases. They are distinguished by time reversal symmetry and the phase winding number N (see Fig. 1). The A-phase is a state conserving the time reversal symmetry ($\eta_\theta \neq 0$ and $\eta_r = 0$) and with $N = 0$. Both the A′- and B-phases violate the time reversal symmetry with $N = 0$ and $N = \pm1$, respectively ($\eta_\theta \neq 0$ and $\eta_r \neq 0$).

At $T = T^*$, the A-phase nucleates, corresponding to $\eta_+(r) = -\eta_-(r) \propto \eta_\theta(r)$ according to eq. (4). As a result of the boundary conditions ($\ell_\theta = \infty$), the order parameter $\eta_\theta(r)$ is the largest at the interface $r = R$ and falls off exponentially on the length scale $\xi'(T) \sim |\tau(r \gg R)|^{-1/2}$ with increasing r. Because $N = 0$, the internal phase structure of the p-wave pair wave function yields the phase difference π across a Ru inclusion for the order parameters $\eta_\pm(\boldsymbol{r})$ in eq. (3) (see Fig. 1).

The A′-phase is also in the topological sector of $N = 0$. A second-order transition from the A-phase may lead to this phase at a temperature below T^*. This transition breaks the time reversal symmetry introduced by the continuous appearance of the subdominant component η_r. From eq. (4), we find that the A′-phase breaks the balance between the amplitudes $|\eta_+(r)|$ and $|\eta_-(r)|$ because $\eta_r \neq 0$ and $\eta_\theta \neq 0$. In this way, one of the two order parameters $\eta_\pm(r)$ becomes predominant as the temperature is lowered, and will eventually decide the chirality of the bulk superconducting phase.

In contrast to the A and A′-phases, the B-phase is a state with $N \neq 0$. We distinguish the two degenerate states $\eta_+ \neq$

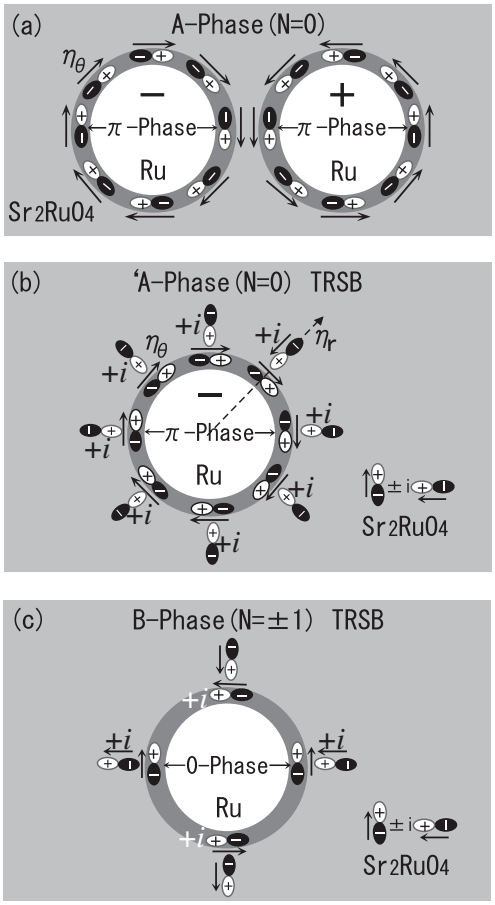

Fig. 1. Topological structure of the A-, B-, and metastable A′-phases. (a) The A-phase corresponds to a time reversal symmetric state with $N = 0$ (winding property). The tangential component of a pair wave function is arranged in such a way as to keep the phase constant around the interface. However, it yields, a diametral phase shift π due to the internal structure of the tangential p-wave state, as indicated in the figure. The perpendicular component vanishes. (b) The A′-phase with $N = 0$ is TRSB due to a finite perpendicular p-wave component. (c) The B-phase is TRSB with $N = \pm 1$ and has a topological structure compatible with that in the bulk phase, $\hat{z}(k_x \pm \mathrm{i}k_y)$.

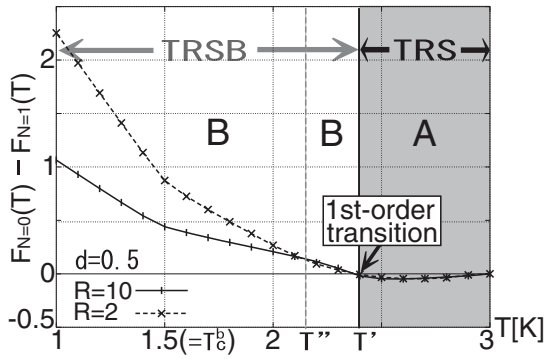

Fig. 2. Temperature dependence of the free energy difference $F_{N=0}(T) - F_{N=1}(T)$ between the states with winding numbers $N = 0$ and 1. The two plots correspond to those in the cases of different-sized Ru inclusions with radii $R = 2$ and 10 in ξ_0 units. The first-order transition from the A-phase ($N = 0$) to the B-phase ($N = 1$) occurs at $T' \approx 2.4\,\mathrm{K}$.

0 and $\eta_- = 0$ with $N = 1$ and $\eta_+ = 0$ and $\eta_- \neq 0$ with $N = -1$. Consequently, the dependence on θ cancels in the representation of the order parameter in eq. (3), unlike the A- and A′-phases. Therefore, this state has the same symmetry and phase topology as the homogeneous bulk phase of Sr_2RuO_4, as can be easily deduced from Fig. 1. Therefore, the B-phase naturally connects to the bulk phase occurring at T_c^b.

In the next step, we examine the sequence of transitions in the temperature range between T^* and T_c^b (Fig. 2). It can be anticipated that below the onset of superconductivity at $T = T^*$, a second transition at a temperature $T = T'$ leads to either the A′-phase or the B-phase. The latter transition (A → B) would be of the 1st order, since it involves a discontinuous change in the winding number ($N = 0 \to N = \pm 1$). In order to determine which of the two states is reached, we have to compare their free energies. The parameters are set to $T_c^b = 1.5\,\mathrm{K}$ of the pure Sr_2RuO_4 and $d = 0.5$ in ξ_0 units in eq. (2). T_0 is adjusted so as to obtain the nucleation temperature for the A-phase to $T^* \approx 3\,\mathrm{K}$. Note that, on a qualitative level, the following results are insensitive to the choice of these parameters.

Our numerical evaluation of the variational equations with the given parameters yields a transition from the A-phase to the B-phase at $T' \approx 2.4\,\mathrm{K}$ (see Fig. 2), which is of the 1st order for the reason discussed above. The continuous transition between the A- and A′-phases has a lower critical temperature ($T'' \approx 2.2\,\mathrm{K}$) and is consequently not realized. We have confirmed that the transition temperature T' shows little sensitivity on the radius R of the Ru inclusion as long as $R \gg 1$ (length unit ξ_0). Therefore, in the case of the single Ru inclusion, we conclude that the first-order transition (A → B) occurs at a temperature below the 3K phase nucleation at $T = T^*$. The B-phase then evolves into the bulk phase at $T = T_c^b$ extending throughout the whole sample.

4. Nature of the Two Phases

In this section, we consider two characteristic properties of the A- and B-phases that can help identify the two phases experimentally.

4.1 Spontaneous currents

We may physically distinguish the A-phase from the B-phase by the fact that the latter carries a spontaneous current that flows along the interface. This is a consequence of the TRSB, while the change in the topology of the states ($N = 0 \to N = \pm 1$) is less important in this context.[5] The expression of the supercurrent is easily derived from the GL free energy [eq. (1)] by using the derivative with respect to the azimuthal vector potential. In the present cylindrical geometry, the radial component of the supercurrent vanishes for symmetry reasons. The azimuthal component is given as

$$j_\theta(r) = \frac{2}{r}\left[(N+1)\eta_+^2(r) + (N-1)\eta_-^2(r) - N\eta_+(r)\eta_-(r)\right] - \eta_-(r)\frac{\partial \eta_+(r)}{\partial r} + \eta_+(r)\frac{\partial \eta_-(r)}{\partial r}. \quad (6)$$

Obviously, this current vanishes in the A-phase where $N = 0$ and $\eta_+ = -\eta_-$. In the B-phase, on the other hand, current flows near the interface. Note that the expression of the current in eq. (6) and the numerical result shown in Fig. 3 do not include the screening effects (i.e., the vector potential is not determined self-consistently). The Meissner–Ochsenfeld screening is of minor importance here since the bulk of the

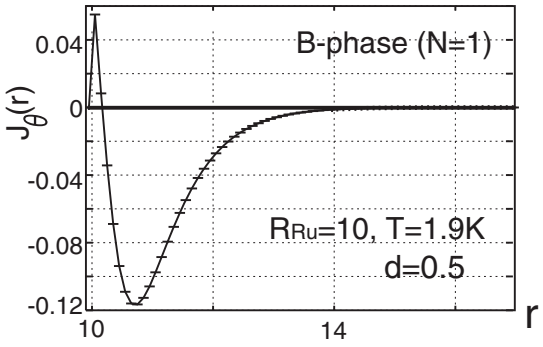

Fig. 3. Spontaneous current around a Ru inclusion in the B-phase originating from the TRSB at $T = 1.9\,\mathrm{K}$ above T_c^b. The radius of the Ru inclusion is $R = 10$ and the interface is located at $r = 10$ in ξ_0 units. Meissner–Ochsenfeld screening is not included in this result.

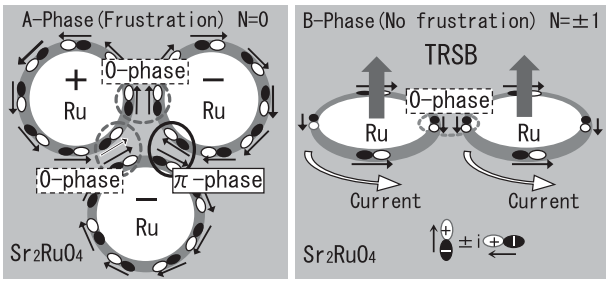

Fig. 4. Inhomogeneous systems with multiple Ru inclusions. Frustration occurs in the A-phase (left panel), while no frustration occurs in the B-phase (right panel). Spontaneous currents in the B-phase have the same circular orientation.

material is not superconducting. The currents are rather small and sparse so that it would be difficult to directly observe the magnetic field generated by those currents, for example, by scanning SQUID or Hall probes. Moreover, the observation of the magnetic fields by means of μSR zero-field relaxation rate measurements is likely difficult owing to the small volume fraction. Below, we will discuss that critical current measurements may be viewed as evidence of the realization of phase transition below T^*, which leads to a TRSB state.

4.2 Coupling between inclusions

Some eutectic Sr_2RuO_4–Ru samples contain regions with a rather high density of Ru inclusions. In these systems, superconducting condensates nucleating at the interfaces of neighboring inclusions can overlap, if they are separated by a length on the order $\xi \sim \xi_0/\sqrt{|\tau|}$ only. A composite of many inclusions can form a superconducting network in the 3K phase whose properties are influenced by the structure of the order parameter on the interfaces. The region of overlapping condensates on neighboring inclusions can be viewed as a weak link or a superconductor/normal metal/superconductor (SNS) Josephson junction. The energetically favored state is realized when the overlapping order parameters have identical phases on both interfaces, as in a standard Josephson junction. For the A-phase condensate, the requirement of identical phases leads to the configurations shown in Fig. 4 (left panel): the p-wave lobes at the closest point align with the same phase ("0-phase") corresponding to parallel arrows for the two upper inclusions in Fig. 4. Such an arrangement leads to the opposite orientation of the arrows winding around these two inclusions.[5)] This is a consequence of the phase structure of the p-wave Cooper pairs. This type of coupling prefers the "+ to −" (winding) configuration of the phases of the superconducting order parameters and, consequently, gives rise to frustration as depicted for the "π-phase" coupling at the lower inclusion in Fig. 4 (left panel), analogous to the case of a triangle of antiferromagnetically coupled Ising spins. It has been earlier speculated that this frustration would yield a non trivial spatial dependence of the order parameter phase and would be visible in the magnetic response of the system, e.g., in ac susceptibility. Thus far, such frustration effects have not been clear observed in experiments.

In contrast to the A-phase, the B-phase has the property in which neighboring inclusions with overlapping condensates would energetically prefer a configuration where both interfaces carry a state of the same chirality, as shown in Fig. 4 (right panel). This ferro-like coupling does not lead to frustration. The spontaneous supercurrents around the inclusions have the same circular orientation, corresponding to a "ferromagnetic" coupling of the orbital moments as the stable configuration. Therefore, the transition between the A- and B-phases also influences the network properties, removing order parameter phase frustrations. In particular, we expect that the circular currents could introduce magnetic flux in the voids of the network, which may be interesting for the response of the system as well as the critical current.

5. Signature of the T'-Transition in Critical Current Measurements

In this section, we address the question of how the transition between the A- and B-phases can be observed experimentally. Since both phases are filamentary, thermodynamic bulk properties such as specific heat would unlikely provide a sufficiently large signal that is measurable. Interestingly, the supercurrents carried by the network of filamentary condensates turn out to give a probe for a transition within the 3K phase. Recent experiments actually gave evidence of a qualitative change in the critical current at $T = 2.3\,\mathrm{K}$.[11)] To explain this finding, we assume that the superconducting network percolates and can carry a very small but finite supercurrent through the sample. Some essential properties of the current flow in such a network are captured by a simple model configuration composed of one loop formed by superconducting paths, as shown in Fig. 5. The important feature of such a SQUID-like structure [Fig. 5 (lower panel)] is the multiple connectivity that makes the current flow susceptible to magnetic fluxes threading the network.

In our "network" the supercurrent splits into two branches, i.e., 1 and 2, corresponding to upper and lower rows of Ru inclusions, respectively, in Fig. 5 (upper panel). For our SQUID-model, we assume each of these two branches as single Josephson contact with its specific sin-like current phase relation:

$$I = I_1 + I_2 = I_{c1}\sin\phi + I_{c2}\sin(\phi + \alpha), \tag{7}$$

where we characterize the branches by their intrinsic critical currents I_{c1} and I_{c2}. These describe the effective current

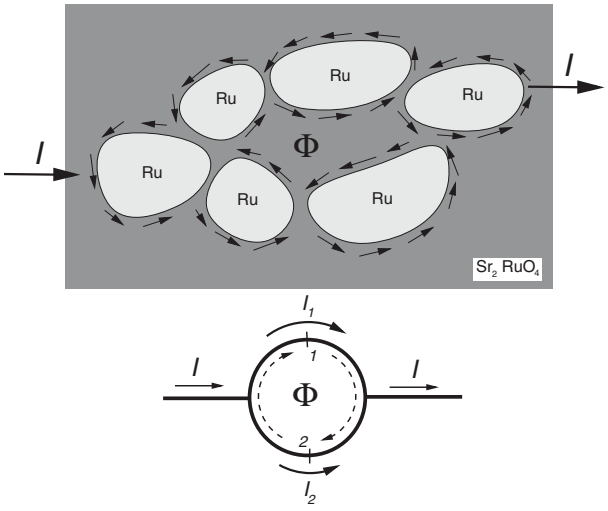

Fig. 5. Simple SQUID network model. Upper panel: The superconducting network formed by the condensates around Ru inclusions, as depicted here, can be viewed as a multiply connected system where the supercurrent can branch and flow in different paths. Lower panel: The configuration of the upper panel can be modeled as a SQUID-like system with two branches, which incorporates the essential features of a network. Note that, in the B-phase, spontaneous currents flow around each inclusion with the same circular orientation such that a net flux occurs through the loop.

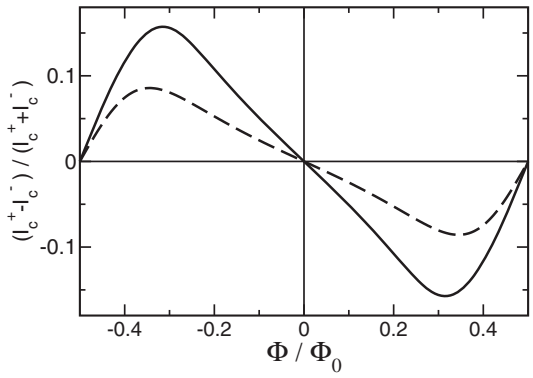

Fig. 6. Difference between the critical currents for opposite directions of I: I_c^+ and I_c^- for critical currents in positive and negative directions, respectively. The plots have been taken using the parameters, $I_{1c}/I_{2c} = 4$ and $LI_{1c}/\Phi_0 = 0.1$ (solid line) and 0.05 (dashed line).

phase relation in the two chains of the Ru inclusions in Fig. 5 (upper panel). The phase coherence of the superconducting order parameter is described by the phases ϕ and α where the latter takes into account the phase difference along the two branches due to the magnetic flux Φ enclosed in the loop, given in a simple effective form as

$$\alpha = \frac{2\pi}{\Phi_0}[\Phi + L(I_1 - I_2)]. \tag{8}$$

Note that Φ represents the magnetic flux induced not only by external magnetic fields, but also by spontaneous currents running along the Sr_2RuO_4–Ru interfaces in the B-phase. These spontaneous currents are not included in the Josephson currents, as they need not to pass between Ru inclusions. The second term represents the contribution to the flux due to the Josephson currents running through the network, specifically through the two arms of the SQUID structure, with L as an effective self-inductance. For simplicity, we assume the two arms to be symmetric in geometry such that their contributions to the induction are identical with opposite signs, while the Josephson coupling strengths are different for the two arms ($I_{c1} \neq I_{c2}$) in order to introduce asymmetry necessary to avoid the cancelation of the current-induced contribution to α.

Now we consider the measurement of the critical current in this network, which corresponds to the maximal supercurrent that can be transfered from one end to the other. In the time-reversal-invariant A-phase, spontaneous currents and flux Φ are absent ($\Phi = 0$). Obviously, the maximal current which can flow through the SQUID network is independent of current direction, as can be easily verified from eqs. (7) and (8), because the reversal of current $I \to -I$ is implemented by $\phi \to -\phi$ leading to $I_i \to -I_i$ ($i = 1, 2$).

In contrast, in the B-phase, spontaneous supercurrents at the interfaces of Ru inclusions generate a finite flux Φ in the loop, which remains basically unaffected by the small Josephson currents. Thus, the analysis of our model shows an explicit symmetry breaking for the current reversal $I \to -I$. The change in the sign of ϕ does not lead anymore to a reversed current in the SQUID, because the flux Φ is fixed in the TRSB phase. Together with the contribution of the current induced flux, this leads to the effect that the maximal current I becomes direction-dependent. Φ determines the magnitude of the critical current difference that changes sign at $\Phi = n\Phi_0/2$, as shown in Fig. 6.

In their experiment, Hooper *et al.*[11] found that the critical current for given contacts does not depend on the orientation of the current flow above $T \approx 2.3$ K. However, below 2.3 K, a finite difference continuously appears for supercurrents flowing in the positive or negative direction. This is in good qualitative agreement with our simple network model.

6. Conclusions

In this study, we investigated the phase diagram of the 3K phase of eutectic Sr–$2RuO_4$–Ru samples, where superconductivity nucleates on the interface of Ru metal inclusions. For a single Ru inclusions, we find a sequence of two phases. At $T^* \approx 3$ K, a time-reversal-symmetry-conserving phase (A-phase) nucleates on the interface. At a lower temperature T', a transition to a time-reversal-symmetry-breaking phase (B-phase) appears. This transition is discontinuous (weakly first order) because the A- and B-phases have different phase winding numbers at a closed (cylindrical) interface. In contrast to the A-phase, the B-phase carries spontaneous supercurrents at the interface due to the TRSB. These currents are most likely responsible for the anomalous behavior of the critical current, which is different for positive and negative current directions, as observed in an experiment below 2.3 K.[11] Thus, we propose to identify the onset of this anomalous behavior as the transition between the A- and B-phases. Further experiment on the quasiparticle tunneling that finds the onset of zero-bias anomalies in the tunneling spectrum below 2.4 K also indicates a phase transition within the 3K phase.[8–10] This behavior also fits well within our phase diagram and will be discussed in detail elsewhere.

Acknowledgment

We are grateful to H. Yaguchi, Y. Maeno, H. Monien, D. F. Agterberg, P. A. Frigeri, T. Ziman, T. Nakamura, R. Nakagawa, T. Yamagishi, and S. Yonezawa for helpful discussions. H.K. is grateful for hospitality of the Pauli Center of ETH Zurich. The numerical calculations were carried out on SX8 at YITP, Kyoto University. This work is supported by the CASIO Science Promotion Foundation, the Hayashi Memorial Foundation for Female Natural Scientists, the Japan Securities Scholarship Foundation, the Japan Science and Technology Agency (JST), and the Swiss Nationalfonds and the NCCR MaNEP.

1) A. P. Mackenzie and Y. Maeno: Rev. Mod. Phys. **75** (2003) 657.
2) Y. Maeno, H. Hashimoto, K. Yoshida, S. Nishizaki, T. Fujita, J. G. Bednorz, and F. Lichtenberg: Nature **372** (1994) 532.
3) Y. Maeno, T. Ando, Y. Mori, E. Ohmichi, S. Ikeda, S. NishiZaki, and S. Nakatsuji: Phys. Rev. Lett. **81** (1998) 3765.
4) H. Yaguchi, M. Wada, T. Akima, Y. Maeno, and T. Ishiguro: Phys. Rev. B **67** (2003) 214519.
5) M. Sigrist and H. Monien: J. Phys. Soc. Jpn. **70** (2001) 2409.
6) M. Matsumoto, C. Belardinelli, and M. Sigrist: J. Phys. Soc. Jpn. **72** (2003) 1623.
7) Z. Q. Mao, K. D. Nelson, R. Jin, Y. Liu, and Y. Maeno: Phys. Rev. Lett. **87** (2001) 037003.
8) M. Kawamura, H. Yaguchi, N. Kikugawa, Y. Maeno, and H. Takayanagi: J. Phys. Soc. Jpn. **74** (2005) 531.
9) H. Yaguchi, K. Takizawa, M. Kawamura, N. Kikugawa, Y. Maeno, T. Meno, T. Akazaki, K. Semba, and H. Takayanagi: J. Phys. Soc. Jpn. **75** (2006) 125001.
10) H. Yaguchi, K. Takizawa, M. Kawamura, N. Kikugawa, Y. Maeno, T. Meno, T. Akazaki, K. Semba, and H. Takayanagi: AIP Conf. Proc. **850** (2006) 543.
11) J. Hooper, Z. Q. Mao, K. D. Nelson, Y. Liu, M. Wada, and Y. Maeno: Phys. Rev. B **70** (2004) 014510.
12) M. Tinkham: *Introduction to Superconductivity* (McGraw-Hill, 1996) 2nd ed., Sect. 4.2.
13) M. Sigrist and K. Ueda: Rev. Mod. Phys. **63** (1991) 239.